

2-D HEAT DIFFUSION IN NUMERICALLY SHOCKED ORDINARY CHONDRITES. J. Moreau¹, S. Schwinger². ¹Department of Geosciences and Geography, University of Helsinki, Finland (juulia.moreau@helsinki.fi), ²German Aerospace Center (DLR), Berlin, Germany.

Introduction: Numerical modeling of shock melting in ordinary chondrites [1-3] hinted that shock-darkening (the melting and spreading of iron sulfides and metals into cracks between silicates) might require heat diffusion to explain the observed metal melting. Indeed, numerical models, using the iSALE shock physics code [4], show that contrasts of post-shock temperatures between iron sulfides, or silicates, and metals are often high (>400 K, [2]), but the code does not consider heat diffusion. Therefore, iSALE models [1-3] produced metal melting only due to sudden rises of pressures or crushing of pores and could not replicate melting of metals in eutectic mixtures with iron sulfides (see Fig. 1, melt fraction), or melting of metals with silicates (e.g. albite) often observed in shocked ordinary chondrites. To study further the melting of phases in shocked ordinary chondrites, we will transfer and diffuse the 2-D temperature maps from iSALE numerical models, used in [2] or [3], and update the melt fraction of phases accordingly.

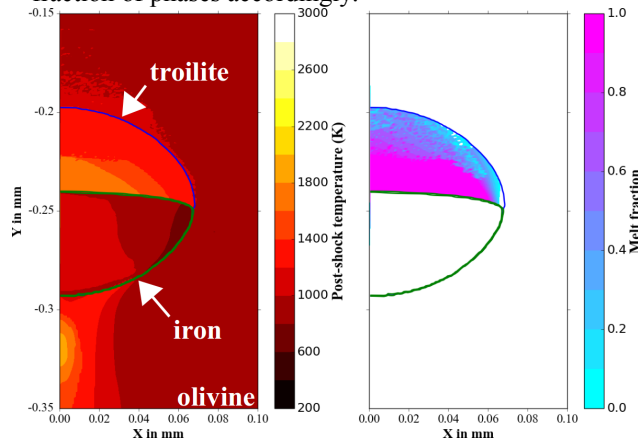


Fig 1. Initial iSALE output for temperatures and melt fractions for the presented model. The model is specifically shown in a compressed state, which does not apply for the diffusion code.

Methods: We built the heat diffusion code using a 2-D finite difference solution for multi-phase meshes (olivine, iron, troilite) with the following characteristics:

- (1) Dirichlet boundary conditions taken from mean values of the iSALE model edges
- (2) update of individual phase heat diffusivities at each time step according to current local temperatures
- (3) consideration of partial melting (using melt fraction, F) with change of state (solid to partial melting, partial melting to complete melting...), without any increase of temperatures during partial melting (heat of fusion).

For simplification, the code only considers these conditions, for now:

- (a) post-shock heat diffusion only, without consideration of heat diffusivity change with pressure, and fixed heat diffusivity at temperatures above the melting point
- (b) even-spaced nodes of different materials (identical to the uncompressed state of the iSALE model material meshes) with no consideration of silicate porosity in treating diffusivity
- (c) simplified eutectic properties (same melting temperatures of 1261 K for iron or troilite phase in mixtures or contact)

The heat diffusivity as a function of temperature for iron and olivine is taken from [5] and [6], respectively. The heat diffusivity of troilite was estimated using changes of heat conductivity with temperature as seen in iron [7], applying the initial heat conductivity of troilite from [8] and the change of heat capacity over temperature for troilite from [9].

Results: As an example, we used a model where a half grain of troilite is atop a half grain of iron in an olivine matrix (model no. 8 from [2]). Initial conditions derived from shock compression are shown in Fig. 1. Iron and troilite have eutectic properties. In Fig. 2 we show results after 300 μ s diffusion time. The major observations, related to the strong temperature contrast between iron and troilite (Fig. 1) are:

- (1) Iron, which was initially solid (Fig. 1), started to heat (Fig. 2b-c) and melt completely at the contact zone with troilite to a distance of 0.02 mm away from it (Fig. 2a).
- (2) Troilite shows a sharp internal temperature contrast (at $y \sim -0.16$ mm, Fig. 2a) that results from a local contrast in shock compression (shock wave reflection from iron, [2]). Relaxation of this temperature contrast leads to a slight increase in melt fraction (from $F=0.63$ to $F=0.70$). As time progresses, troilite cools by diffusing heat towards the much colder phases surrounding it.
- (3) The variations of temperatures and melt fractions are reduced rapidly by thermal equilibration, with initial temperature contrasts between metal and troilite progressively reduced.

Discussion and conclusions: As mentioned in [2,3], heat diffusion must be considered as a trigger for melting iron or other phases in order to explain melt features in ordinary chondrites that could not be replicated with the iSALE models for shock compression. Thus,

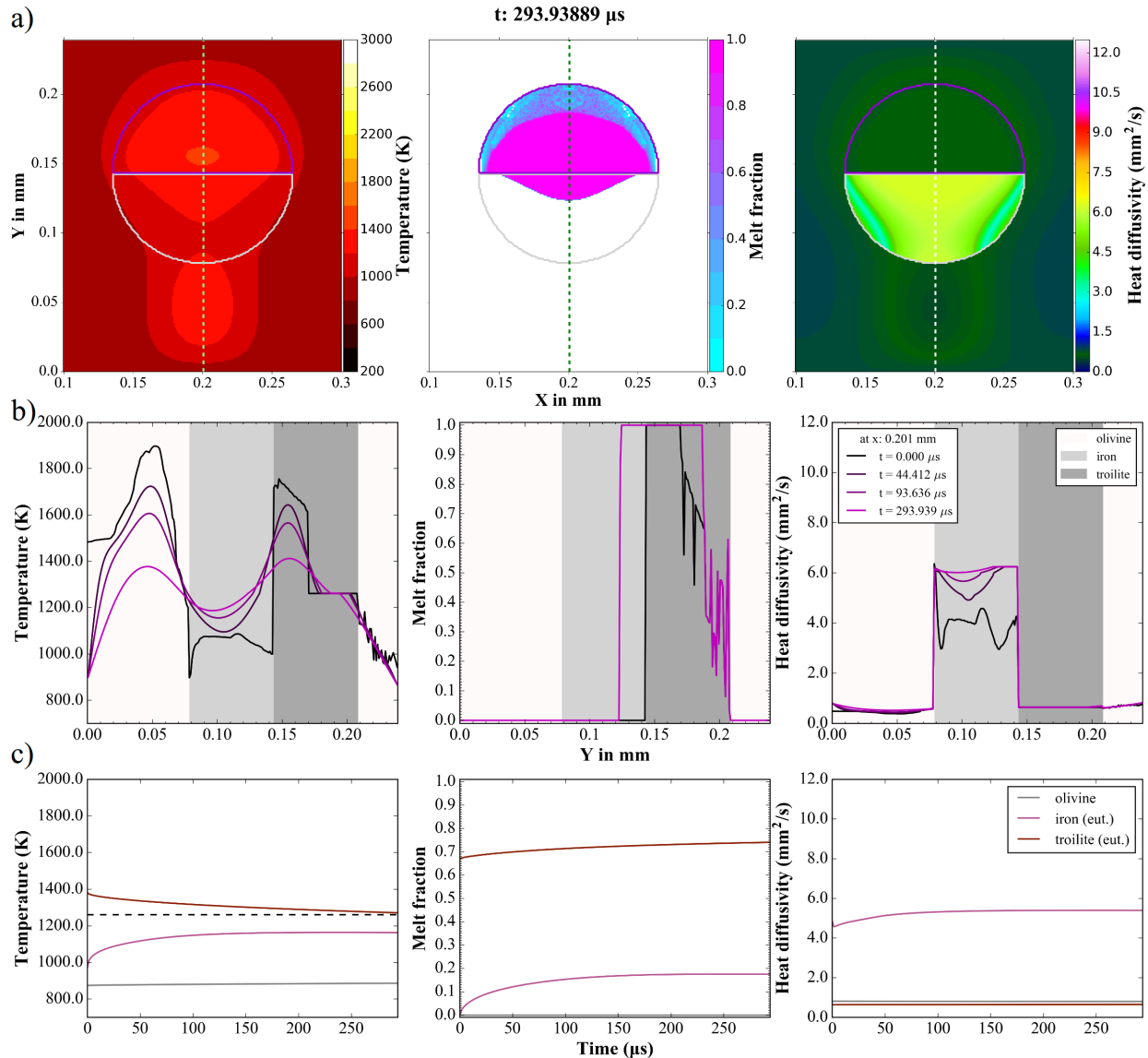


Fig 2. Temperatures, melt fractions and diffusivities with: a) 2-D distribution after 300 μs of heat diffusion, b) cross-section profiles, at chosen time steps, at $x: 0.130 \text{ mm}$ as shown in a) by dashed lines, c) variation over time for the individual materials (mean values of the whole material bulk). Troilite is delineated in purple and iron is delineated in light gray in a). Eutectic melting temperature is indicated in c) by dashed line.

offering the possibility to diffuse heat after shock will give a better estimate of the production of melt in shocked ordinary chondrites either from shock or from post-shock heat diffusion. Finally, considering the time scales of heat diffusion, an evaluation of heat diffusion effects might also require further consideration of the duration of shock compression, which depends on the scale of the impact (e.g. 100-1000 μs in collisions between asteroids or $<1 \mu\text{s}$ in shock-recovery experiments [10]).

Acknowledgements: Our thanks to the iSALE developers, and Lars Kaislaniemi for sharing the idea for the diffusion code. This work is supported by the Academy of Finland and by the Deutsche Forschungsgemeinschaft (SFB-TRR170, subproject C4) and the

Helmholtz association (project VH-NG-1017).

References: [1] Moreau J. et al. (2017) *Meteorit. Planet. Sci.*, 52(11), 2375-2390. [2] Moreau J. et al. (2018). *Phys. Earth Planet. In.*, 282, 25-38. [3] Moreau J. et al. (2018). *Icarus*, submitted. [4] Wünnemann K. et al. (2006) *Icarus*, 180, 514-527. [5] Monaghan B. J. and Queded P. N. (2001) *ISIJ Int.*, 41(12), 1524-1528. [6] Gilbert B. et al. (2005) *Phys. Earth Planet. In.*, 151, 129-141. [7] Abu-Eishah S. I. (2001) *Int. J. Thermophys.*, 22(6), 1855-1868. [8] Yomogida K. and Matsui T. (1983) *J. Geophys. Res.*, 88(B11), 9513-9533. [9] Chase Jr. M. W. (1998) NIST-JANAF thermochemical tables, monograph. In: *J. Phys. Chem. Ref. Data.*, 1-1951. [10] Moreau J. et al. (2018) *EPSC 2018*, vol. 12, abstract #212.